Summer Student Programme 2021

Radiation protection for ion therapy centre, simulations using Monte-Carlo with SRIM

Deianira Fejzaj, *University of Brescia*, Brescia, Italy

Mentor: Mimoza Ristova, *University Ss Cyril and Methodius,* Skopje, North Macedonia

Table of Contents

1. Introduction

1.1 General overview of Hadron therapy (particle therapy)

The goal of particle therapy is to exploit the possibility of depositing a high dose in the *target* volume (usually the tumor) with a minimum dose in the surrounding healthy tissue. To achieve this goal, use is made of the characteristic shape of the dose profile deposited by the particles as a function of depth: a plateau followed by a peak (the so-called *Bragg peak*) and a drop to zero just before the end of the range. The irradiation is performed by 'filling' the target volume with Bragg peak doses. The particle energy determines the depth at which the Bragg peak dose will be deposited in the patient's body. The clinically useful maximum beam energy for proton therapy is 200–250 MeV. For carbon ions, the maximum energy used is 400–450 MeV per nucleus. The lowest particle energies which are down to a few megaelectron volts are needed for treatment of very superficially located tissues. Today all particle treatments are done with beams of protons or carbon ions [1].

Carbon-ion beams have gained a strong interest because they exhibit Bragg peak in the body, followed by rapid dose fall-off beyond the peak, enabling delivery of sufficient dose to the target volume while minimizing the dose to the surrounding tissues. Furthermore, as compared with proton beams, carbon-ion beams cause less scattering and range-struggling in the body [*2*].

Radiation protection is a key aspect of any radiotherapy (RT) department; in Ion Beam Therapy (IBT) large and complex radiation producing devices are used and made available to the public for treatment. It is thus the responsibility of the facility to put in place measures to protect not only the patient but also the general public, occupationally and non-occupationally exposed personnel working within the facility, and electronics installed within the department to ensure maximum safety.

The purpose of this study is to propose a radiation protection shielding (maze) made of sandwich walls composed of concrete walls with soil in between. This work will present the analysis of the shielding in case of dumping the direct proton or ion-beam into the maze wall. The analysis will be made using Monte Carlo simulations from the SRIM package.

2. Materials and Methods

2.1 Physical aspects for using ions in therapy [3]

When photons of short wavelengths (X- or gamma rays) strike condensed matter, they release electrons from the atoms they interact with. Due to the statistical nature of the absorption process and the fact that photons are strongly deflected (scattered) during their interactions with atoms, a photon beam entering condensed matter spreads rapidly and has no defined range. In contrast to the indirectly ionizing electromagnetic radiation, radiation consisting of charged particles (electrons, alpha particles, accelerated ions) is directly ionizing.

In classical mechanics, the transfer of kinetic energy is inversely proportional to the square of the velocity v ($dE/dx \sim 1/v^2$). Due to their low mass, accelerated electrons reach rapidly high velocities close to the speed of light (at energies > 1 MeV). As the electron velocity approaches the speed of light c, the energy loss per unit length becomes independent of the energy ($dE/dx \sim 1/c^2$). As a consequence, relativistic electrons deposit a constant energy dose per unit length. The low mass renders electrons subject to strong lateral scattering.

For protons and all heavier ions, because of their much higher mass, ions experience significantly less lateral scattering than electrons (proton-to-electron mass ratio is 1.836:1). Accelerated atomic nuclei of the therapeutically relevant kinetic energy (approx. 40–400 MeV/u) interact predominantly via Coulomb forces with the target electrons of the traversed matter. This leads to excitation and ionization of atoms along the track of the traveling particle. Quantitatively, the energy loss per unit path length, also called stopping power, of these heavy charged particles is described by the Bethe formula:

$$\frac{dE}{dx} \sim \frac{K n_0 {Z_{eff}}^2}{\beta^2 [ln\left(\frac{2 m_e c^2 \beta^2}{I(1-\beta^2)}\right) - \beta^2]} \qquad (1)$$

where K is a constant, n_0 the electron density of the target material, Z_{eff} the effective charge of the projectile ions, β the velocity of the projectile in units of the speed of light ($\beta = v/c$), I the mean ionization energy of the target atoms, and m_e the rest mass of the electron.

Together, these effects produce the sharp rise and fall at the end of the ion track – the Bragg peak – in the graphical representation of energy loss or relative dose as function of penetration depth. Most ion particles travel the same distance in a monoenergetic beam. But not all experience the same number of collisions. Their range is, therefore, somewhat different. This phenomenon is called straggling.

2.2 Radiation shielding basics

Shielding for an Ion Beam Therapy (IBT) facility must address both the primary particles (protons, carbon ions, etc.) and the secondary particles produced from the ions interacting with beam line components and the patient [4]. The secondary particles of primary concern when constructing shielding for the facility are neutrons and photons. Both often have a large range, and in the case of neutrons, high quality factors for biological damage [5].

The choice of shielding materials is complex as the shielding material itself has a direct impact on secondary particle production. Case in point, as the mass number of the target/shield increases, the total neutron yield increases, yet the ability to absorb photons also increases. For IBT facilities the target is the patient which has a low mass number and a low neutron yield. Other components of the beam line such as the passive scattering system and beam collimation system have a higher mass number and, subsequently, yield a higher number of neutrons that may be shielded to minimize the dose received by humans [4].

Most shielding is designed using various Monte Carlo (MC) modeling programs and then verified using a range of radiation metrology techniques.

Traditionally the three main materials used in IBT facility shielding are earth, concrete and steel. These materials offer good shielding characteristics, while also being cost effective for large facilities with multiple treatment rooms.

The SiO_2 content of soil also makes it effective in shielding neutrons and photons. Concrete is another shielding material that is used in facility shielding based on cost and the ease in which it can be poured into the desired shapes and thicknesses. In addition, concrete offers the added benefit of its structural strength. Most modern vaults or treatment rooms utilize concrete extensively as a shielding material. One disadvantage of concrete is that naturally occurring sodium within the concrete can become activated from interactions with the primary beam, potentially increasing the background radiation levels in the accelerator and treatment areas from the shielding itself. To limit increases in background radiation from primary beam interactions, low-sodium concrete or the addition of boron compounds have been used. Steel can also be used as a shielding material, however, steel alone can cause a buildup of low-energy neutrons and is usually used in conjunction with concrete.

2.2.1 Setting up a shield using SRIM package

For the purpose of evaluating a bunker for radiation protection this study utilizes the SRIM package (SRIM and TRIM) to perform Monte-Carlo simulations. TRIM or Transport of Ions in Matter is a Monte-Carlo computer program that calculates the interactions of energetic ions with amorphous target using several physical approximations while still maintaining accuracy [6]. In this case, the target is a bunker for radiation protection, also called a shielding, is constructed of walls made of concrete and soil. The 1D cross-section model of the sandwich walls is shown in Figure 1.

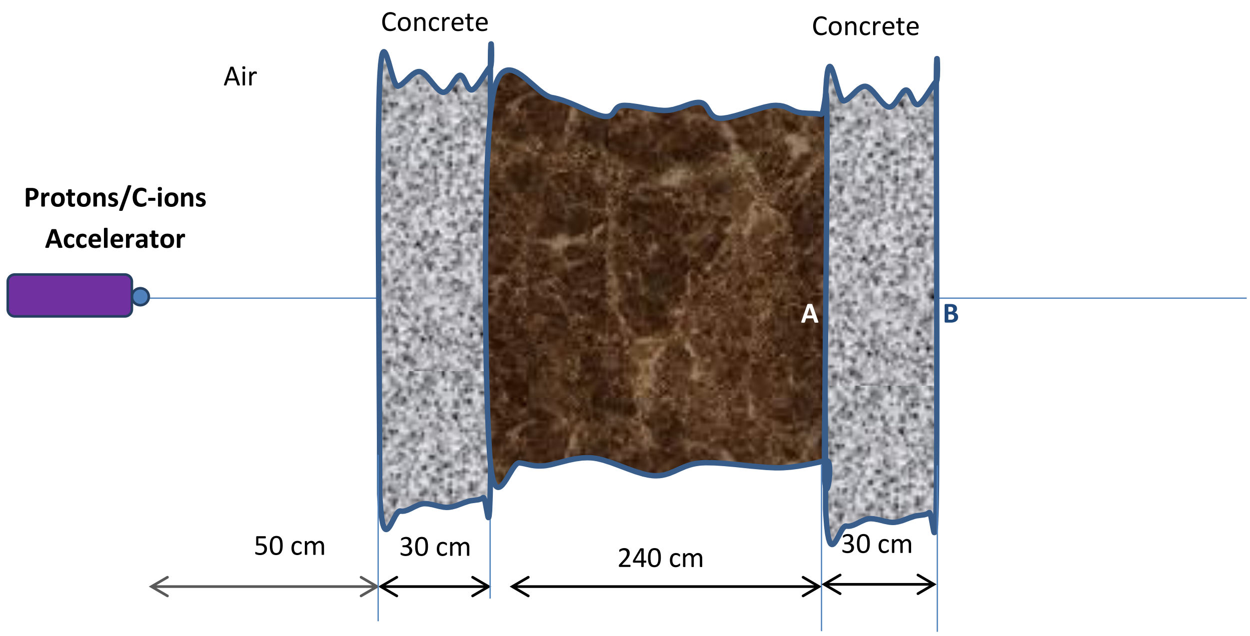

Figure 1. Model of the bunker to be analyzed for radiation protection.

The purpose of shielding is to stop all the irradiated ions or protons coming from the accelerator. It is needed to evaluate until which point do the ions penetrate the shield. Firstly, it is considered point A shown in Figure 1 and then point B.

For the study it is necessary to set the target, which is made of compounds of elements represented with a certain stoichiometry. It is also essential to set the total number of ions in the beam, which in our case is rather low due to weak PC performances, -999999.

In target layers are inserted the materials (the compounds, taken directly from the TRIM library of materials, except for the soil) which compose the bunker. As it was mentioned before, the shielding thickness goes until the point A along the accelerated particle direction.

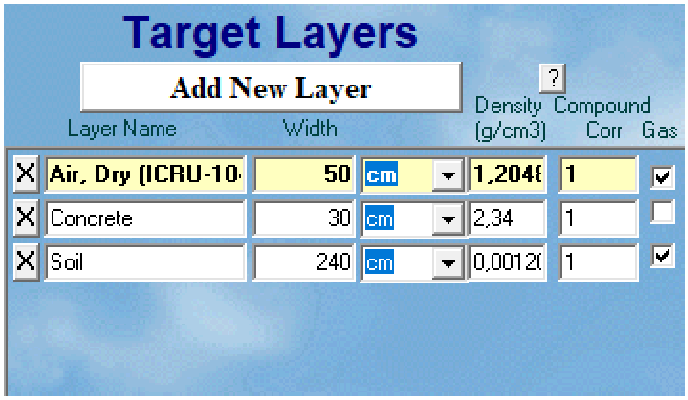

Figure 2. Set-up of TRIM target

In Figure 2 it is shown the final view of the layer; each component can be directly taken from SRIM library (Compound Dictionary -> Common Target Materials) or may be inserted manually. In this case, the air layer and concrete layer are taken from the library. Herein the layer of soil with its elemental content, stoichiometry and density were set manually. In TRIM, the width of the target is calculated as a sum of each layer and it equals to 320 cm.

2.3 Stochiometric analysis for the concrete, soil and dry air target

Based on the model of the bunker shown in Figure 1 and the target shown in Figure 2, it is proceeded with the calculations and finding the atomic stoichiometry and the density of each of these layers.

The concrete's stoichiometry is $C_{23}\,O_{40}\,Si_{12}\,Ca_{12}\,H_{10}\,Mg_{2}$ and it is given in the SRIM library along with the density ρ=2.34±0.15 g/cm^3. In Table 1 it is calculated the weighted fraction of each element in the dry concrete.

Table 1. Calculated number of atoms of each element in 1 cm^3 dry concrete assuming $C_{23}\,O_{40}\,Si_{12}\,Ca_{12}\,H_{10}\,Mg_{2}$ stoichiometric compound and density ρ=2.34±0.15 g/cm^3.

Elements in Concrete (dry)	At. Number	At. Mass [g/mol]	Stoichiometry (Number of atoms in compound)	Mass per element in the compound	Wt. fraction of each element in the compound	Mass of each element in 1 cm^3 concrete [g]	n (# of moles of each element in 1 cm^3 concrete	Number of atoms in 1 cm^3
C	6	12	23	276	0.154	0.361	0.030	1.811E+22
O	8	16	40	640	0.358	0.837	0.052	3.149E+22
Si	14	28	12	336	0.188	0.439	0.016	9.446E+21
Ca	20	40	12	480	0.268	0.627	0.016	9.446E+21
H	1	1	10	10	0.006	0.013	0.013	7.872E+21
Mg	12	24	2	48	0.027	0.063	0.003	1.574E+21
							0.129	
SUM (total molecular mass)				1790	1	2.34		7.793E+22

The same calculations are made with the soil assuming soil assuming $C_{135}N_{22}O_{529}Mg_{20}Al_{83}Si_{190}K_8Ca_{13}$ stoichiometric compound and density ρ=1.6 g/cm^3.

Table 2. Calculated number of atoms of each element in 1 cm^3 dry concrete assuming $C_{135}N_{22}O_{529}Mg_{20}Al_{83}Si_{190}K_8Ca_{13}$ stoichiometric compound and density ρ=1.6 g/cm^3.

Elements in Soil	At. Number	At. Mass [g/mol]	Stoichiometry (Number of atoms in compound)	Mass per element in the compound	Wt. fraction of each element in the compound	Mass of each element in 1 cm^3 concrete [g]	n (# of moles of each element in 1 cm^3 concrete	Number of atoms in 1 cm^3
C	6	12	135	1620	0.084	0.134	0.011	6.752E+21
N	7	14	22	308	0.016	0.025	0.002	1.100E+21
O	8	16	529	8464	0.439	0.703	0.044	2.645E+22
Mg	12	24	20	480	0.025	0.039	0.002	1.001E+21
Al	13	27	83	2241	0.116	0.186	0.007	4.151E+21
Si	14	28	190	5320	0.276	0.442	0.015	9.502E+21
K	19	39	8	312	0.016	0.026	0.001	4.001E+20
Ca	20	40	13	520	0.026	0.043	0.001	6.502E+20
							0.083	
SUM (total molecular mass)				19265	1			5.001E+22

The dry air composition it is directly taken from the SRIM package, (Compound Dictionary -> Common Target Materials) with the stoichiometry as $O_{23.2}$ $N_{75.5}$ $Ar_{1.3}$ and density ρ= 0.00120484 g/cm^3. In Table 3 it is calculated the weighted fraction of each element in the dry concrete. The carbon is not shown in stoichiometry of SRIM (because it is only 0.015%) but its value is considered in the compounds of the target.

Table 3. Calculated number of atoms of each element in 1 cm^3 dry concrete for dry air.

Elements in Soil	At. Number	At. Mass [g/mol]	Stoichiometry (Number of atoms in compound)	Mass per element in the compound	Wt. fraction of each element in the compound	Mass of each element in 1 cm^3 concrete [g]	n (# of moles of each element in 1 cm^3 concrete	Number of atoms in 1 cm^3
C	6	12	0.015	12.015	0.066	7.953E-05	6.627E-06	3.991E+18
O	8	16	23.2	39.2	0.215	0.0002	1.622E-05	9.766E+18
N	7	14	75.5	89.5	0.492	0.0006	4.232E-05	2.548E+19
Ar	18	40	1.3	41.3	0.227	0.0003	6.834E-06	4.115E+18
							7.2E-05	
SUM (total molecular mass)				182.015	1	0.0012		4.335E+19

2.4 Applying a proton beam and C-beam in the target

Based on the settings of the TRIM program in section 2.2.1, the application produces as an output the ion distribution for a beam of hydrogen ions (protons) and a beam of carbon ions, the ion ranges (parameter and plot) and the ionization plot.

The ranges of ion are calculated using the transport equation approach developed by J. P. Biersack, which he called PRAL (Projection RAnge ALgorithm). This method allows the rapid calculation of ion ranges over a large band of ion energies. The ranges are quite accurate, usually within 5% if those found using TRIM (which is the most accurate method of calculating ranges). The range straggling values are less accurate and are tabulated for reference [6].

2.4.1 Proton Beam

The ions data are set entering the ion name (H in this case) or clicking the PT for obtaining the periodic table of the elements. The ion energy is set at 0.5 GeV. There is no need for an angle of incidence. The type of TRIM calculation it is set as "Ion Distribution and Quick Calculation of Damage" since it is needed to calculate the final distribution of ions in the target and the ionization energy loss by the ion into the target.

In Figure 3 it is shown the plot of ion distribution with recoils projected on XY-plane where X is the depth axis. As it can be noted, the X axis is the target's size (320 cm or 3.2 m as it is shown in the figure).

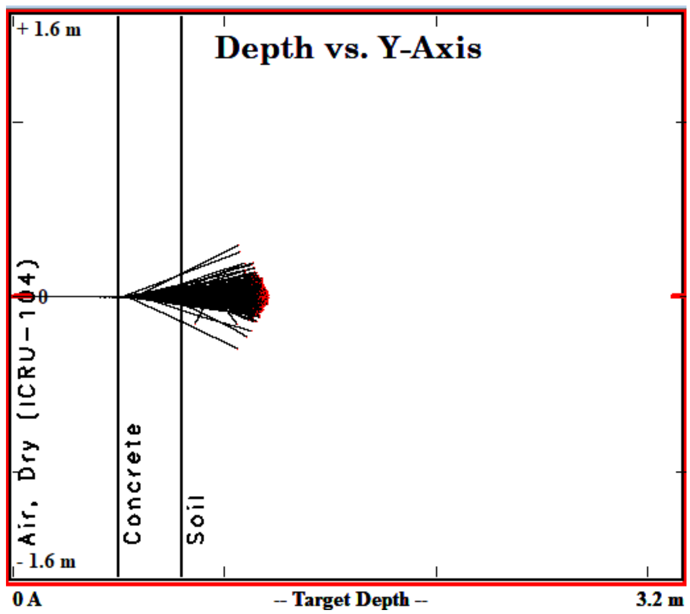

Figure 3. Proton's distribution on XY plane.

From the calculation parameters it was obtained the Ion Stats as it shown in Table 4.

Table 4. Ion Stats: output parameters from TRIM simulation for H ions in the target.

	Range	**Straggle**
Longitudinal projection	1.17 m	10.4 mm
Lateral projection	11.9 mm	16.9 mm
Radial projection	18.7 mm	14.9 mm

According to the Table 4, the proton beam outputs the three-dimensional distribution of the ions in the solid and its parameters, such as penetration depth that is the Range parameter. In this case the ions penetrate the shield until 1.17 m along the X-axis (Longitudinal projection). The spread of the ions, along the ion beam and perpendicular to it, it is called Straggle as it is also mentioned in section 2.1.

2.4.2 Carbon ions Beam

The ions data are set entering the ion name (C in this case) or clicking the PT for obtaining the periodic table of the elements. The ion energy is set at 0.5 GeV. There is no need for an angle of incidence. The type of TRIM calculation it is set as "Ion Distribution and Quick Calculation of Damage" since it is needed to calculate the final distribution of ions in the target and the ionization energy loss by the ion into the target. In Figure 4 it is shown the plot of ion distribution with recoils projected on XY-plane where X is the depth axis.

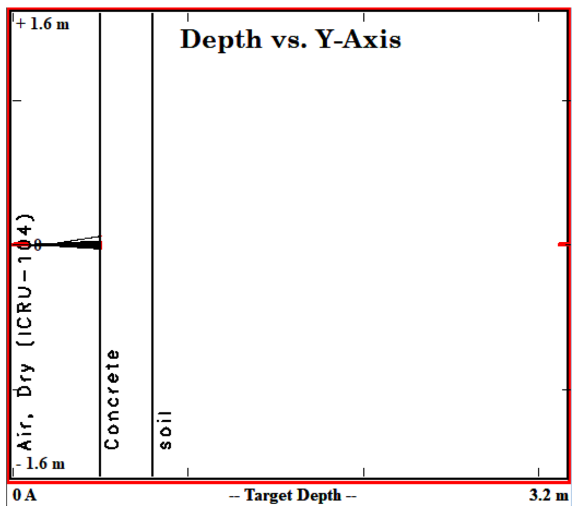

Figure 4. Carbon ions' distribution on XY plane.

From the calculation parameters it was obtained the Ion Stats:

Table 5. Ion Stats: output parameters from TRIM simulation for C ions in the target.

	Range	Straggle
Longitudinal projection	502 mm	1.39 mm
Lateral projection	579 um	1.62 mm
Radial projection	913 um	1.71 mm

According to the Table 5, the carbon ion beam penetrates the target with a depth of 502 mm along the X-axis.

3. Results and discussion

Proton beam

The Figure 5 represents the Ion distribution in 2D and 3D. The "ion ranges" is the distribution of the protons (500 MeV) building up in the compound target [6]. The range is 1.17 m. the target depth is 3.2 m and it is seen a gap of 2.03 m between the point A of the shield and the ion range.

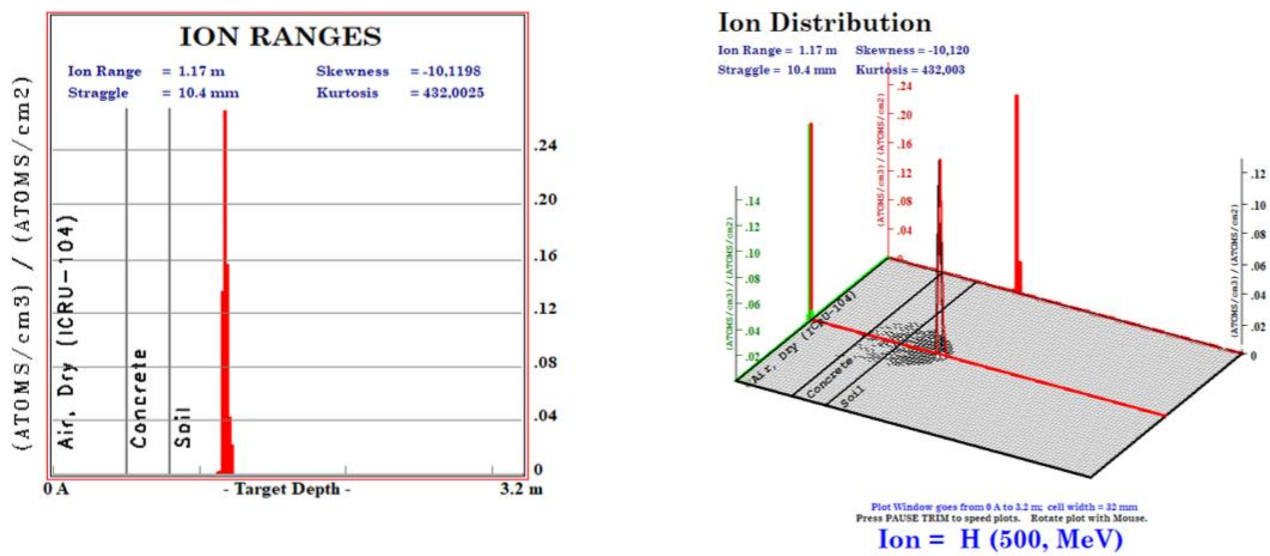

Figure 5. Ion distribution in 2D (left) and 3D (right).

The abscissa shows the depth in the target, and the ordinate has units of (Atoms/ cm^3) / (Atoms/ cm^2). The ordinate is set so that by multiplying by an ion-beam dose, normally in units of "Atoms/ cm^2", the plot reads directly as a concentration in units of ***atoms/*** $\mathbf{cm^3}$. In this case is circa 0.24 (Atoms/ cm^3) / (Atoms/ cm^2) [6].

In Figure 6 is plotted the spatial distribution of the Ionization and it shows the energy dissipated to target electrons. According to the plot, the energy loss to electrons is by direct interaction with ions (99.98% of energy). The ionization contribution from recoils is only 0.01% and therefore it is not displayed. It is noticed that the energy is dissipated more in the soil target. The energy loss in the highest peak at the depth of circa 1.17m is 0.18 eV/Ang.

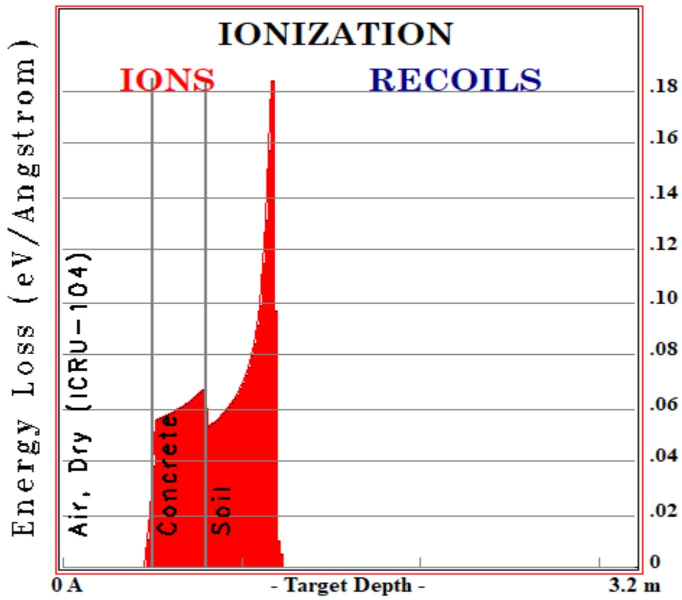

Figure 6. Ionization plot for protons in target.

Carbon ion beam

The Figure 7 represents the Ion Ranges which is the distribution of the carbon ions (500 MeV) building up in the compound target. The ion range is 502 mm. the target depth is 3.2 m and it is seen a gap of 2.68 m between the point A of the shield and the ion range.

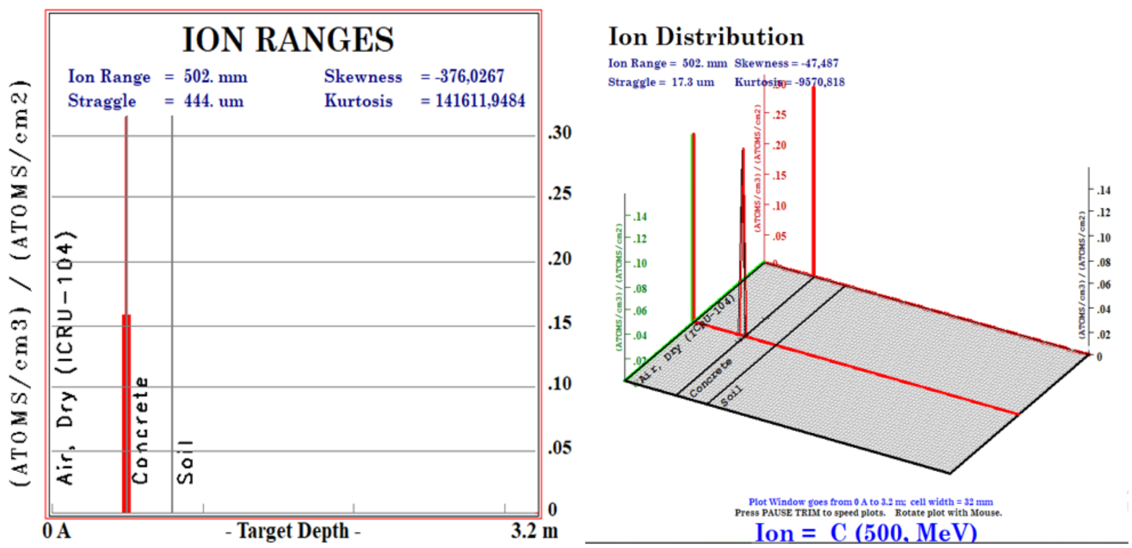

Figure 7. Ion distribution in 2D (left) and 3D (right).

The same considerations are made as in the proton's case.

The Figure 8 is the Ionization, and it shows the energy dissipated to target electrons. It is noticed that all the energy is dissipated in the concrete target's surface. The highest peak is more than 1.4 eV/Ang at depth of circa 502 mm.

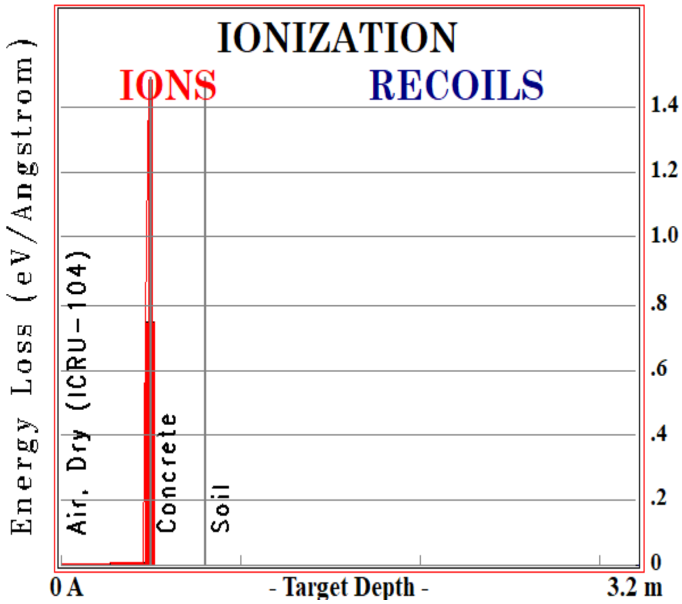

Figure 8. Ionization plot for carbon ions in target.

The results show that the carbon ions with same energy as the protons have a smaller depth of penetration than the protons (both accelerated at 500 MeV). This is understandable because the carbon ions are 12 times heavier than the protons. So, the shield for carbon ions can be shorter compared to the shield for the protons.

Another analysis it is made for the ionization and ion range of the protons and carbon ions in concrete (depth 30 cm) with energy ranging from 100 MeV to 1 GeV.

For the carbon ions, the Ion Ranges distribution is plotted in Figure 9.

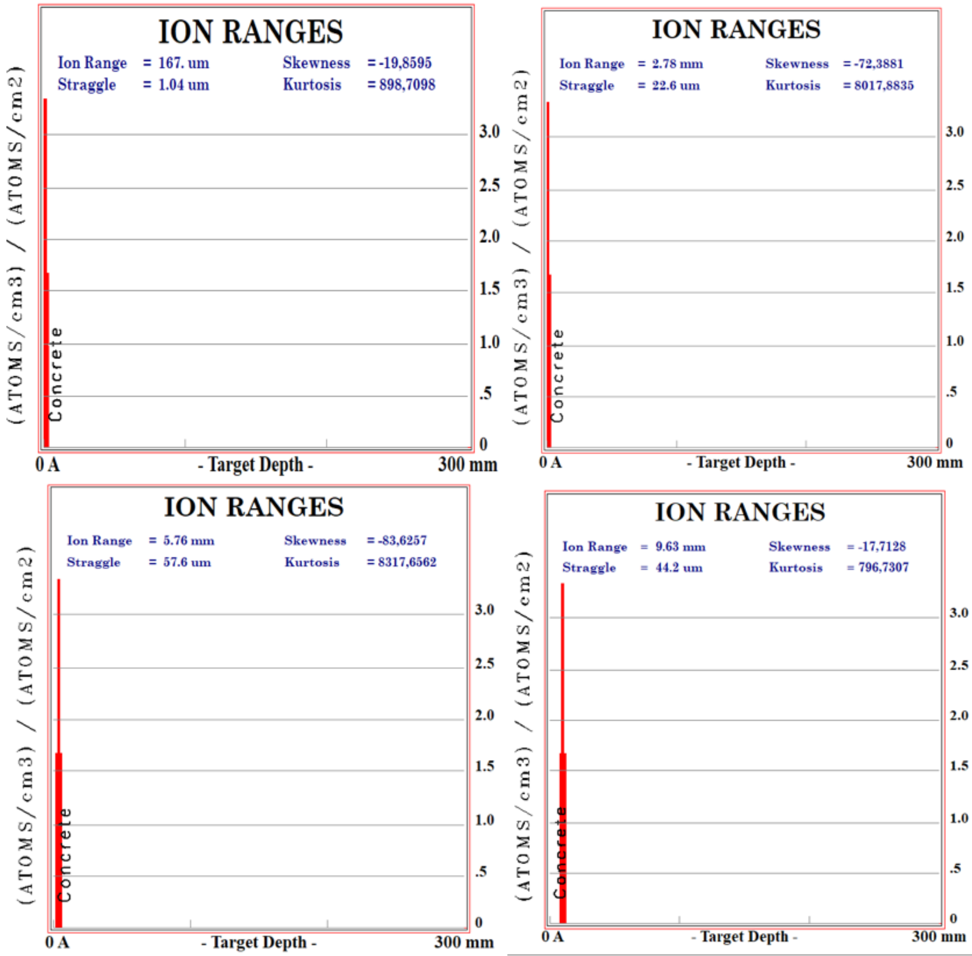

Figure 9. Ion ranges plot for carbon ions at 100 MeV (upper left), 500 MeV (upper right), 750 MeV (down/left) and 1 GeV (down-right).

From the results obtained it is shown that increasing the energy of the ion beam, it increases the ion range; in other words, the carbon ions at higher energy penetrate deeper in the target. The range is shown in Table 5.

Table 4. Carbon energy vs Depth in concrete (ion range).

Carbon energy [MeV]	**Depth in the concrete target [mm]**
100	0.167
500	2.78
750	5.76
1000	9.63

Also, the ionization as it is shown in Figure 10:

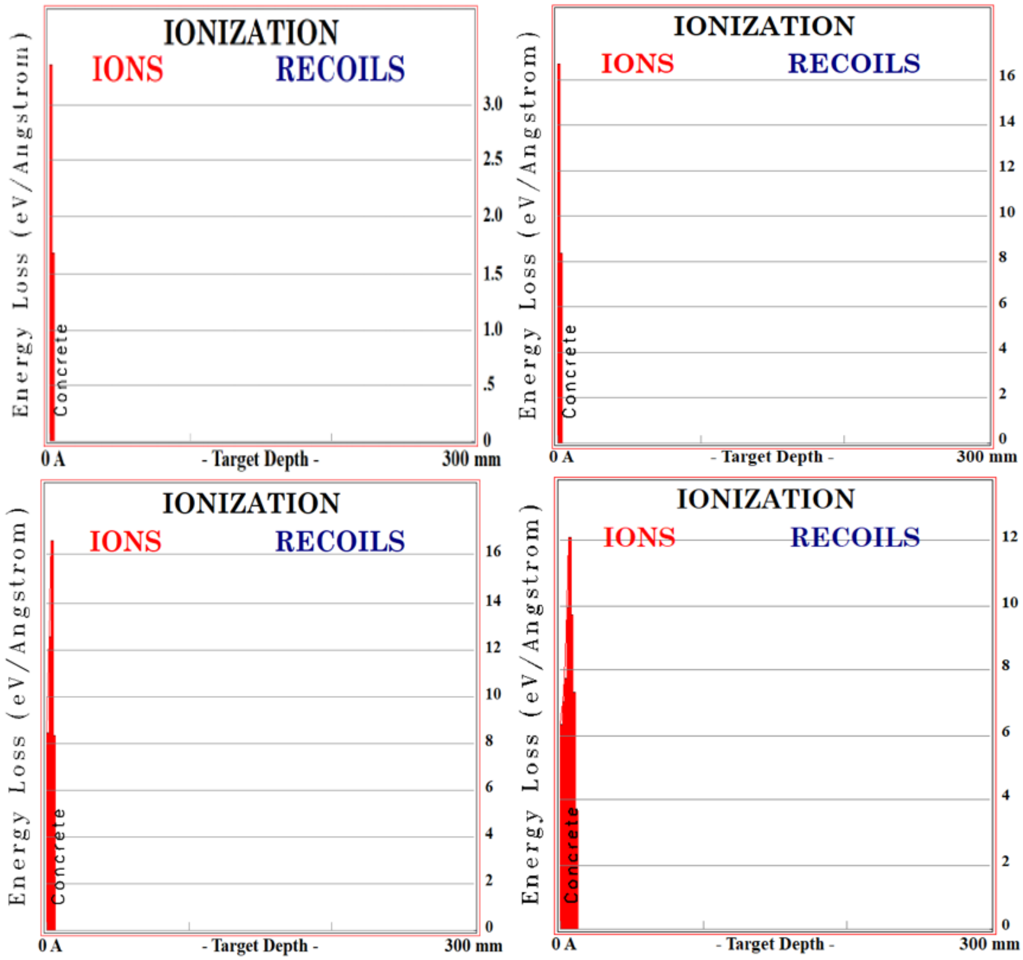

Figure 10. Ionization plot for carbon ions at 100 MeV (upper left), 500 MeV (upper right), 750 MeV (down/left) and 1 GeV (down-right).

For the protons, the Ion Ranges distribution is plotted in Figure 11.

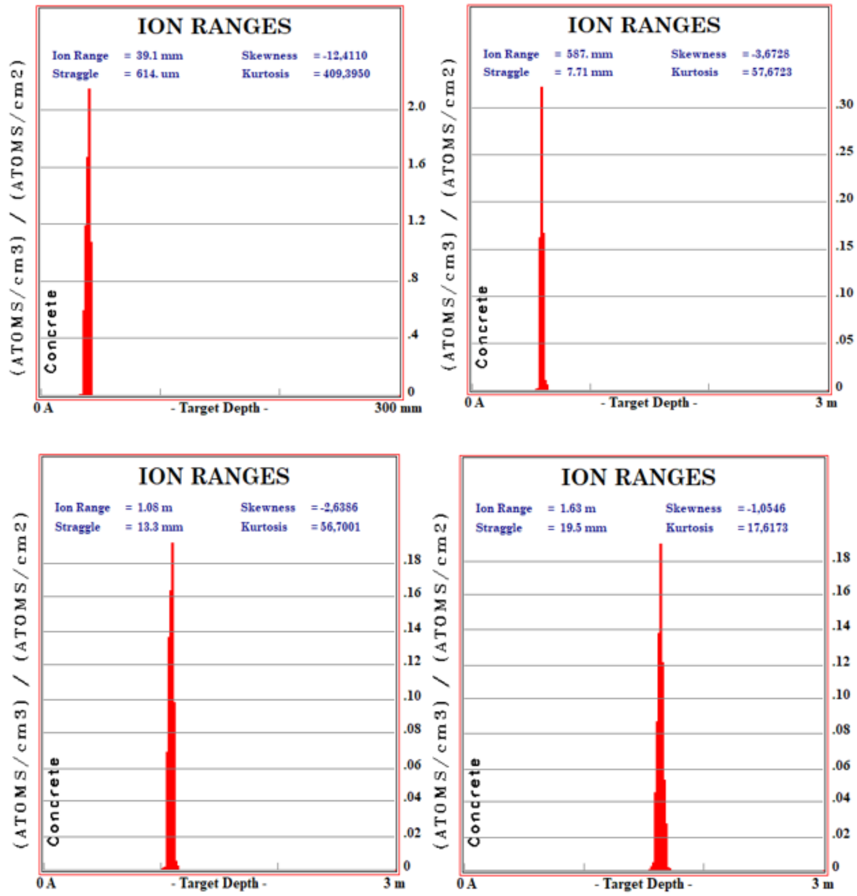

Figure 11. Ion ranges plot for protons at 100 MeV (upper left), 500 MeV (upper right), 750 MeV (down/left) and 1 GeV (down-right).

From the results obtained it is shown that increasing the energy of the ion beam, it increases the ion range; in other words, the protons at higher energy penetrate deeper in the target. The range is shown in Table 5.

Table 5. Proton energy vs Depth in concrete (ion range).

Proton energy [MeV]	**Depth in the concrete target [mm]**
100	39.1
500	587
750	1080
1000	1630

Also, the ionization, as it is shown in Figure 12:

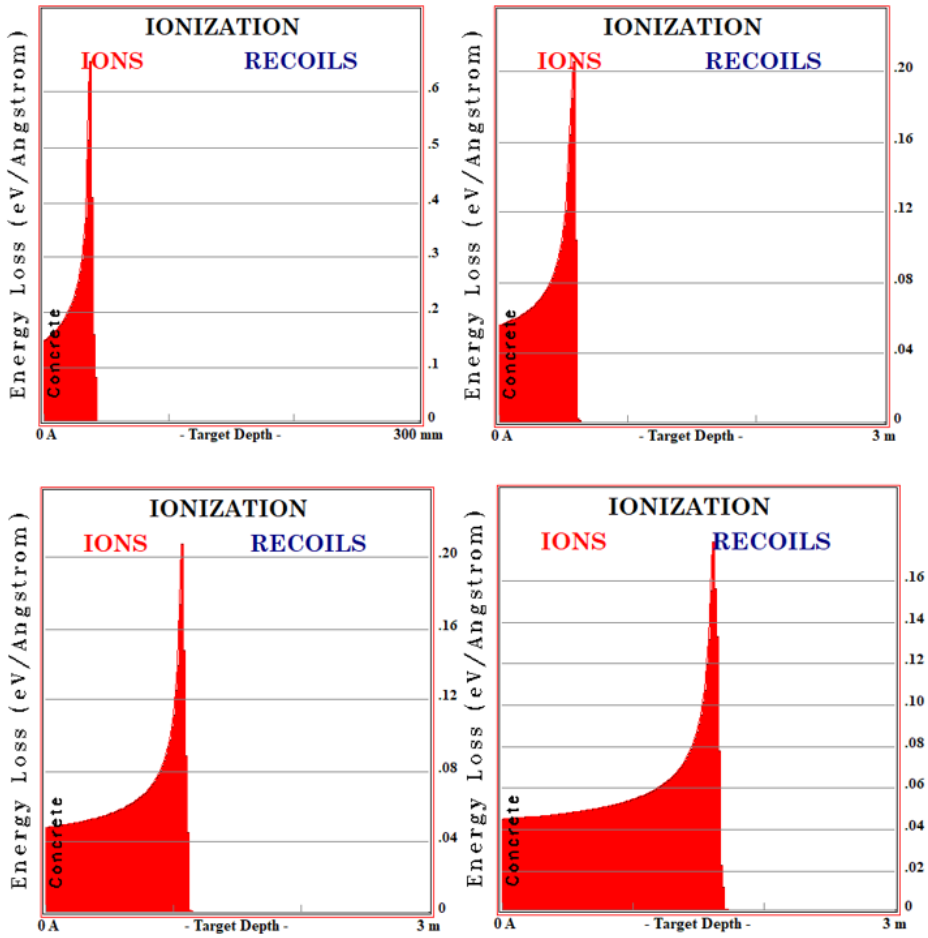

Figure 12. Ionization plot for carbon ions at 100 MeV (upper left), 500 MeV (upper right), 750 MeV (down/left) and 1 GeV (down-right).

The Figure 13 shows the plot of Energy vs Depth in target of the beams (proton and c-ions) with the data obtained from Table 5 and Table 6.

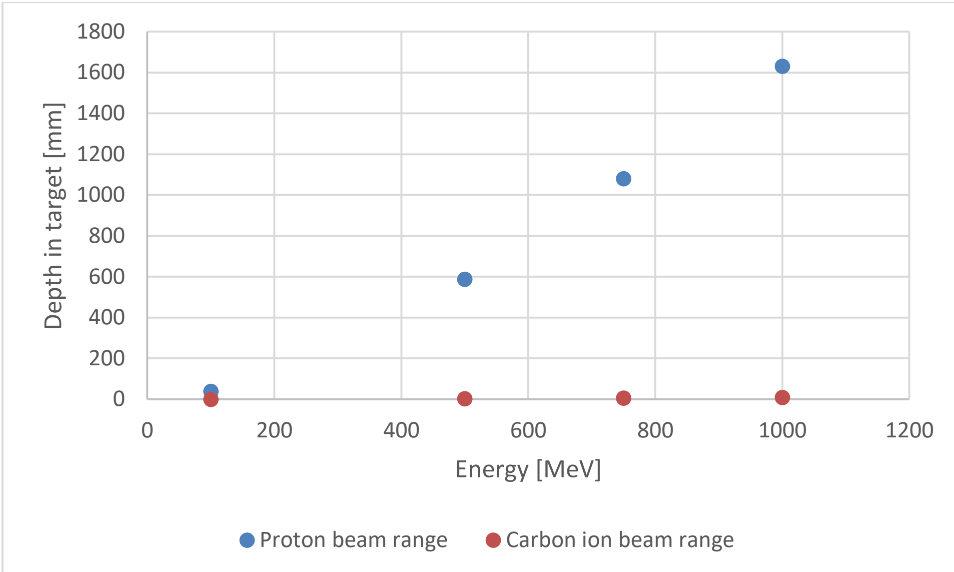

Figure 13. Energy vs Depth in target.

As it can be seen from the plot, the carbon ions' function is "constant" compared to protons. This happens because the protons, with the increasing energy, go much deeper in the target compared to carbon ions. It is also good to mention that for calculating the ion range in proton's case, the concrete's width must be increased (with 500 MeV the width of target had to be increased). So, for protons at high energy it is needed a wider shield compared to the shield needed for carbon ions.

4. References

[1] M. Schippers *Advances in Beam Delivery Techniques and Accelerators in Particle Therapy*

[2] H. Tsujii and T. Kamada *Overview of Carbon-Ion Radiotherapy in Japan*, National Institute of Radiological Sciences National Institute for Quantum and Radiological Sciences, Chiba, Japan

[3] U. Linz. *Physical and Biological Rationale for Using Ions in Therapy*

[4] A. J. Wroe, S. Rightnar. *Shielding and Radiation Protection in Ion Beam Therapy Facilities*

[5] National Council on Radiation Protection and Measurement. *Protection Against Neutron Radiation* (NCRP Report 38, Bethesda, MD, USA, 1971)

[6] J. F. Ziegler and J. P. Biersack and M. D. Ziegler (2008). *SRIM - The Stopping and Range of Ions in Matter.* SRIM Co. ISBN 978-0-9654207-1-6.